Fuel-Optimal Trajectory Planning of Satellites Using Minimum Distance Assignment and Comparative Analysis of Relative Dynamics under J2 and Air Drag

Himadri Basu, Yasaman Pedari, Mads Almassalkhi, Hamid R. Ossareh

Abstract— **In this paper, we present a fuel-optimal trajectory optimization (TO) problem for satellite formation flying (SFF) in near-circular low-earth orbits (LEO) under perturbations and modeling uncertainties. Non-spherical gravity (J2) of the earth and air drag are two dominant perturbing forces in LEO which cause significant orbital measurement errors and eventually sub-optimal actuation and trajectory prediction by the TO algorithm. By quantifying uncertainties and modeling errors associated with various relative dynamical models of satellites, we identify a model that is suitable for the TO problem. However, one of the key challenges to design of a computationally efficient TO algorithm for satellite swarms pertains to the assignment of each satellite to a location in a given final formation. To address this, we first decouple the final configuration assignment problem from the TO, derive minimum distance assignment between initial and final formation pairs, and then by using this minimum distance assignment in the TO algorithm, we efficiently compute near-optimal trajectories and actuation under given mission specifications. We validate all the theoretical results with suitable numerical examples.**

I. Introduction

Formation flying spacecraft in LEO has been a subject of active research in the last decade because of its potential applications in performing complex missions, such as distributed imaging of earth's surface, atmospheric sampling, and interferometry at reduced costs, increased flexibility, reconfigurability and performance compared to a monolithic spacecraft [1]. The primary goal of satellite formation flying (SFF) [2] is to place a cluster of cooperative satellites into nearby orbits to achieve a group objective.

SFF missions typically require complex reconfiguration maneuvers such as moving, reorienting, and rotating a fleet of spacecrafts from an initial configuration to a desired target configuration [3]. It is important to carry out these maneuvers in a fuel-optimal manner while satisfying physical and mission-specific constraints. Fuel/time-optimal control of spacecraft formation based on linear programming was presented in the works of [3]–[5] and with nonlinear programming in [2]. In general, SFF with small formation size has been studied well in the literature. Interested readers, please refer to [6], [7] and references therein. However, in [2], [4], [5], relative dynamical model of satellites used in the TO does not take into account the effects of J2 gravity, which is the most dominant source of perturbation [8], [9]. Additionally, the nonconvex optimization constraints in [2] make the TO algorithm computationally hard and inapplicable for practical missions (especially when computations are to be carried out by the onboard processors). In contrast to these works, our objective in this paper is to propose a computationally efficient, scalable TO framework which devotes due consideration on modeling accuracy of satellites in LEO, capturing the effects of both the J2 perturbation and air drag with sufficient accuracy.

In circular LEO around a perfectly spherical and homogeneous earth, the Hill-Clohessy-Wiltshire (HCW) equations are shown to be good linear approximations of the relative dynamics in [10], [11]. In reality, because of the non-uniform gravitational pull of the earth due to its oblateness (i.e., J2 effects), the HCW models may not be applicable in all SFF missions [12]. Furthermore, in LEO, the air resistance is strong enough to produce a drag modifying the semi-major axis and eccentricity over a sufficiently long period of time [13]. There are several relative dynamical models proposed in the literature, *e.g.* [14], [15], under various assumptions and methodologies, which consider either or both of these effects. A high fidelity nonlinear model considering the effects of J2 drift was developed in [16] for a formation keeping problem, which was later extended to include the effects of air drag in [1]. As the model's complexity hampers its application in control designs [12], we present here a comparative analysis of various dynamical models. By quantifying modeling errors, we identify an appropriate model specific to LEO SFF mission design.

Specifically, in this work, we revisit four relative dynamical models - namely: (i) high fidelity nonlinear model in [1] that considers both the effects of J2 and air drag, (ii) linearized J2 model in [16], (iii) Hill's equations in [10], (iv) Modified Hill's equations with J2 in [11]. To select an appropriate model for TO, we first compare relative dynamical models (ii)-(iv), stated above, with respect to the high fidelity nonlinear model (i) and compute modeling errors for various initial conditions. This analysis has not been conducted in a cohesive manner before, and modeling errors have not been formally quantified. We fill this gap and quantify the errors, which allows us to identify the linearized J2 as an excellent candidate to be used as computationally simple state-space constraints in the TO problem.

One of the main challenges in designing a computationally

The authors are with the Department of Electrical and Biomedical Engineering, University of Vermont, Burlington, VT 05405, USA. Email: himadri.basu@uvm.edu, yasaman.pedari@uvm.edu, malmassa@uvm.edu, hossareh@uvm.edu.

This work was supported by NASA under cooperative agreement VT-80NSSC20M0213.

efficient TO algorithm is the assignment of satellites in a fuel-optimal configuration on the final formation. Given a set of positions and velocities on a final formation of the satellite swarm, the objective of this assignment problem is to assign each satellite to a specific final destination in a way that is fuel optimal for the entire fleet. We present here an alternative approach to decouple the final configuration assignment problem from the trajectory optimization problem to make this more computationally tractable at the expense of a small loss (at most 10%) in fuel-optimality. To this end, instead of simultaneously finding fuel-optimal final assignment and trajectories, we rather solve separately a "minimum cost transportation problem" to derive the shortest distance assignment between initial and final formation pairs [17]. Then, by using the computed final assignments, we efficiently find alternative near-optimal trajectories and actuation profiles under given mission specifications. The assignment problem can be solved efficiently centrally (e.g., by one of the satellites), while the TO problem can be solved by all satellites in a distributed fashion.

Contributions: In this work, we present a computationally efficient trajectory planning algorithm of SFF, which is appropriate for use in implementation of coordination and control architecture in practical missions. Main contributions are: (1) quantification of uncertainties around different models, and selection of linearized J2 model as suitable relative state-space dynamical system for TO problem, (2) decoupling of assignment algorithm from the TO problem to efficiently compute near-optimal satellite trajectories under given mission specifications.

The organization of the paper is as follows. In Section II, we define the problem statement along with the mission specifications. In Section III, we review various relative dynamical models of satellites, evaluate modeling errors and consequently quantify uncertainties in Section IV. Next, we formulate our minimum fuel TO problem in Section V and with the help of a numerical example we illustrate the shortcomings in the implementation of this basic TO algorithm in practical missions. In Section VI, we present main results containing alternative approaches to reformulate TO for computationally efficient implementation and scalability. All the theoretical developments are validated with accompanying illustrative examples in respective sections. Finally, some concluding remarks and future research directions are given in Section VII.

II. Problem Statement

Given initial and final formation of N identical satellites in close proximity in circular or near-circular LEO subject to J2 gravity and air drag, the objective of this paper is to derive a computationally efficient, scalable TO framework satisfying all physical and mission specific constraints, discussed below, such that all these satellites under predicted actuation from the trajectory planning algorithm, make optimal maneuvers to reach to the final formation after a specified time duration with minimal fuel consumption. The results presented here are relevant for practical space missions related to SAR interferometry, imaging of earth's surface, etc.

As noted above, we consider a homogeneous fleet of satellites equipped with the same actuating thrusters and sensing suites. As a result, it does not matter which satellite ends up in which point of the final formation. Since none of the satellites have a priori knowledge of its destination point on the final formation, we need to not only design a TO but also an assignment problem to assign satellites to their fuel-optimal final points. Furthermore, for general SFF missions, ongoing research emphasizes more on distributed computation of optimal trajectories, actuation, final configuration cooperatively by the satellite swarm with the help of their onboard computers. For a large-scale satellite swarm with simple onboard computers, the central question to address then becomes how can we make our TO, control, and estimation algorithms more computationally efficient so that they meets all the required processing and communication requirements. With this as motivation, in this work we propose alternative approaches to improve the computationally efficiency of the TO algorithm so that it becomes scalable and suitable for practical SFF mission.

Mission specifications: We now summarize below the mission specifications for illustrative numerical simulations presented in this paper. Inspired by a formation flying space mission TechSat-21 [18] by U.S. Air Force Research Laboratory (AFRL) in 2006 and their mission specifications, the position tolerance of the desired relative states in this work are chosen to be 5 m in radial, along-track and across-track directions with respect to the "target orbit", where the term target orbit will be defined formally later. Additionally, in the current SFF mission, we assume that the initial "target orbit" is circular or near-circular and all the satellites are initially located within 15 km from this "target orbit". Each satellite is equipped with three thrusters of 3 mN actuation limits with each pointing respectively in radial, along-track and across-track direction. The robust optimal actuation force, as predicted by the trajectory planner here is applicable to other thruster configurations as well, namely- coupling thrusters and reaction wheels/magnetometers through a lower-level transformation controller.

III. Review of various relative dynamical models of satellites

In this section, we review various relative dynamical models of LEO satellites, capturing primarily the effects of J2 perturbation and air drag. For brevity, through the rest of the paper, we use shorthand notation for trigonometric identities such as $\mathrm{s}_\theta = \sin\theta, \mathrm{c}_\theta = \cos\theta$.

In the traditional texts on dynamical motion of satellites, a virtual unactuated satellite or a fictitious moving point is usually taken as a reference and all N participating satellites in formation as followers. Given the initial orbital elements, the position and velocity vectors of this reference satellite at every time instant define a target orbit. This target orbit is generally expressed in Earth-centered inertial (ECI) coordinate frame which has its origin located at the center of the earth, x axis aligned with earth's mean equator and passes through vernal equinox, z axis along the celestial north pole while the y axis completing the right hand orthogonal frame with the other two [11].

Considering the two main disturbances, namely J2 and atmospheric drag, the differential equations governing the motion [1] of the target orbit are:

$$\dot{r} = v_x, \tag{1}$$
$$\dot{v}_x = -\frac{\mu}{r^2}+\frac{h^2}{r^3}-\frac{K_{J2}}{r^4}(1-3\mathrm{s}_i^2\mathrm{s}_\theta^2)-C\|\mathbf{V}_a\|v_x, \tag{2}$$
$$\dot{h} = -\frac{K_{J2}}{r^3}\mathrm{s}_i^2\mathrm{s}_{2\theta} - C\|\mathbf{V}_a\|(h-\omega_e r^2\mathrm{c}_i), \tag{3}$$
$$\dot{\Omega} = -\frac{2K_{J2}}{hr^3}\mathrm{c}_i\mathrm{s}_\theta^2 - \frac{C\|\mathbf{V}_a\|\omega_e r^2\mathrm{s}_{2\theta}}{2h}, \tag{4}$$
$$\dot{i} = -\frac{K_{J2}}{2hr^3}\mathrm{s}_{2i}\mathrm{s}_{2\theta} - \frac{C\|\mathbf{V}_a\|\omega_e r^2\mathrm{s}_i\mathrm{c}_\theta^2}{h}, \tag{5}$$
$$\dot{\theta} = \frac{h}{r^2} + \frac{2K_{J2}\ \mathrm{c}_i^2\mathrm{s}_\theta^2}{hr^3} + \frac{C\|\mathbf{V}_a\|\omega_e r^2\mathrm{c}_i\mathrm{s}_{2\theta}}{2h}, \tag{6}$$

where r and v_x are respectively the orbital position and velocity in ECI coordinates, h, Ω, i, θ denote angular momentum, right ascension of the ascending node (RAAN), inclination angle and geodesic latitude, $C = 0.5C_d\dfrac{A}{m}\rho$, C_d is air drag coefficient, A/m is the cross-section area of the spacecraft per unit mass, ρ is atmospheric density,

$$\mathbf{V}_a = \begin{bmatrix} v_x & (\frac{h}{r}-\omega_e r\mathrm{c}_i) & \omega_e r\mathrm{c}_\theta\mathrm{s}_i \end{bmatrix}^{\mathrm{T}}$$

is the orbital velocity vector with respect to the atmosphere, $\omega_e = 7.2921\times10^{-5}\ \mathrm{rad\,s^{-1}}$, $\mu = 398600\ \mathrm{km\,s^{-2}}$ is gravitational constant, $K_{J2} = 1.5\mu J_2 R_e^2$ with second zonal harmonic constant $J_2 = 1.082\times10^{-3}$, and earth's mean equatorial radius $R_e = 6378$ km.

The relative dynamical motion of all follower satellites are described in local-vertical-local-horizontal (LVLH) frame [19], with its origin located on the target orbit. In this local coordinate frame, the relative position vector of j^{th} spacecraft is usually expressed as $\bar{\mathbf{r}}_j = \begin{bmatrix} x_j & y_j & z_j\end{bmatrix}^{\mathrm{T}}$ where the unit vectors associated with x_j, y_j and z_j respectively point in the radial, along-track and across-track directions.

A. High fidelity nonlinear relative dynamical model

As described in [1], the equations of motion for j^{th} spacecraft under J2 perturbation and atmospheric drag, relative to the target orbit are given as follows.

$$\begin{aligned}\ddot{x}_j &= 2\dot{y}_j\omega_z - x_j(n_j^2-\omega_z^2) + y_j\alpha_z - z_j\omega_x\omega_z + a_{jx}\\ &\quad -\bar{\zeta}\mathrm{s}_i\mathrm{s}_\theta - r(n_j^2-n^2) - l_{1j}(\dot{x}_j - y_j\omega_z) - l_{2j}v_x, \end{aligned}\tag{7}$$
$$\begin{aligned}\ddot{y}_j &= -2\dot{x}_j\omega_z + 2\dot{z}_j\omega_x - x_j\alpha_z - y_j(n_j^2-\omega_z^2-\omega_x^2)\\ &\quad + z_j\alpha_x - \bar{\zeta}\mathrm{s}_i\mathrm{c}_\theta + a_{jy}, \end{aligned}\tag{8}$$
$$\ddot{z}_j = -2\dot{y}_j\omega_x - x_j\omega_x\omega_z - y_j\alpha_x - z_j(n_j^2-\omega_x^2) - \bar{\zeta}\mathrm{c}_i + a_{jz}, \tag{9}$$

where $l_{1j} = C\|\mathbf{V}_{aj}\|, l_{2j} = C(\|\mathbf{V}_{aj}\| - \|\mathbf{V}_a\|)$, $\bar{\zeta} = \zeta_j - \zeta$, $\mathbf{V}_{aj}$ is the velocity of the j^{th} spacecraft with respect to the atmosphere, a_{jx}, a_{jy} and a_{jz} are control accelerations respectively in x, y, z directions of the LVLH frame,

$$\begin{aligned}
\zeta &= \frac{2K_{J2}\mathrm{s}_i\mathrm{s}_\theta}{r^4}, \zeta_j = \frac{2K_{J2}r_{jZ}}{r^5},\\
n^2 &= \frac{\mu}{r^3} + \frac{K_{J2}}{r^5} - \frac{5K_{J2}\mathrm{s}_i^2\mathrm{s}_\theta^2}{r^5},\\
n_j^2 &= \frac{\mu}{r_j^3} + \frac{K_{J2}}{r_j^5} - \frac{5K_{J2}r_{jZ}^2}{r_j^7},\\
r_j &= \sqrt{(r+x_j)^2 + y_j^2 + z_j^2},\\
r_{jZ} &= (r+x_j)\mathrm{s}_i\mathrm{s}_\theta + y_j\mathrm{s}_i\mathrm{c}_\theta + z_j\mathrm{c}_i.\\
\alpha_z &= -\frac{2hv_x}{r^3} - \frac{K_{J2}}{r^5}\mathrm{s}_i^2\mathrm{s}_{2\theta},\\
\alpha_x &= f_x - \frac{K_{J2}\mathrm{s}_{2i}\mathrm{c}_\theta}{r^5} + \frac{3v_xK_{J2}\mathrm{s}_{2i}\mathrm{s}_\theta}{r^4h} - \frac{8K_{J2}^2\mathrm{s}_i^3\mathrm{c}_i\mathrm{s}_\theta^2\mathrm{c}_\theta}{r^6h^2},\\
f_x &= -C\|\mathbf{V}_a\|\omega_e\left(\frac{2rv_x\mathrm{c}_\theta\mathrm{s}_i}{h} - \left(\frac{r}{h}\right)^2\mathrm{c}_\theta\mathrm{s}_i\dot{h} + g_x\right),\\
g_x &= -\frac{r^2\mathrm{s}_\theta\mathrm{s}_i\dot{\theta}}{h} + \frac{r^2\mathrm{c}_\theta\mathrm{c}_i\dot{i}}{h}
\end{aligned}\tag{10}$$

with $\dot{h}$, $\dot{i}$ and $\dot{\theta}$ being given respectively in (3), (5), (6).

B. Linearized J2 model

In the high fidelity nonlinear model (7) – (10), there are nonlinear terms n_j^2, ζ_j which include polynomials of the reciprocal of r_j and consequently x_j, y_j, z_j. By using Gegenbauer polynomials, the terms n_j^2 and ζ_j were shown to bear a linear relationship in [16] with the decision variables x_j, y_j and z_j as follows

$$\begin{aligned}
\zeta_j &= \zeta - \frac{8K_{J2}x_j\mathrm{s}_i\mathrm{s}_\theta}{r^5} + \frac{2K_{J2}y_j\mathrm{s}_i\mathrm{c}_\theta}{r^5} + \frac{2K_{J2}z_j\mathrm{c}_i}{r^5},\\
n_j^2 &= n^2 - \frac{3\mu x_j}{r^4} - \frac{5K_{J2}}{r^6}\left[x_j(1-5\mathrm{s}_i^2\mathrm{s}_\theta^2) + y_j\mathrm{s}_i^2\mathrm{s}_{2\theta} + z_j\mathrm{s}_{2i}\mathrm{s}_\theta\right].
\end{aligned}$$

With the above substitution, the first order linear J2 model yields the following time-varying dynamics

$$\begin{aligned}\ddot{x}_j &= \frac{2\dot{y}h}{r^2} + x_j\left(\frac{2\mu}{r^3} + \frac{h^2}{r^4} + \frac{4K_{J2}(1-3\mathrm{s}_i^2\mathrm{s}_\theta^2)}{r^5}\right) + a_{jx}\\ &\quad - y_j\left(\frac{2v_xh}{r^3} - \frac{3K_{J2}\mathrm{s}_i^2\mathrm{s}_{2\theta}}{r^5}\right) + \frac{5K_{J2}\mathrm{s}_{2i}\mathrm{s}_\theta}{r^5}, \end{aligned}\tag{11}$$
$$\begin{aligned}\ddot{y}_j &= -\frac{2\dot{x}_jh}{r^2} - \frac{2K_{J2}\dot{z}_j\mathrm{s}_{2i}\mathrm{s}_\theta}{r^3h} + x_j\left(\frac{2v_xh}{r^3} + \frac{5K_{J2}\mathrm{s}_i^2\mathrm{s}_{2\theta}}{r^5}\right)\\ &\quad - y_j\left(\frac{\mu}{r^3} - \frac{h^2}{r^4} + \frac{K_{J2}(1+2\mathrm{s}_i^2-7\mathrm{s}_i^2\mathrm{s}_\theta^2)}{r^5}\right)\\ &\quad + z_j\left(\frac{3K_{J2}v_x\mathrm{s}_{2i}\mathrm{s}_\theta}{r^4h} - \frac{2K_{J2}\mathrm{s}_{2i}\mathrm{c}_\theta}{r^5}\right) + a_{jy}, \end{aligned}\tag{12}$$
$$\begin{aligned}\ddot{z}_j &= \frac{2K_{J2}\dot{y}_j\mathrm{s}_{2i}\mathrm{s}_\theta}{r^3h} + \frac{5K_{J2}x_j\mathrm{s}_{2i}\mathrm{s}_\theta}{r^5} - \frac{3K_{J2}y_jv_x\mathrm{s}_{2i}\mathrm{s}_\theta}{r^4h}\\ &\quad - z_j\left(\frac{\mu}{r^3} + \frac{K_{J2}(3-2\mathrm{s}_i^2-5\mathrm{s}_i^2\mathrm{s}_\theta^2)}{r^5}\right) + a_{jz}, \end{aligned}\tag{13}$$

where r, v_x, h, θ, i are time-varying forcing terms obtained by solving Eqs. (1)–(6).

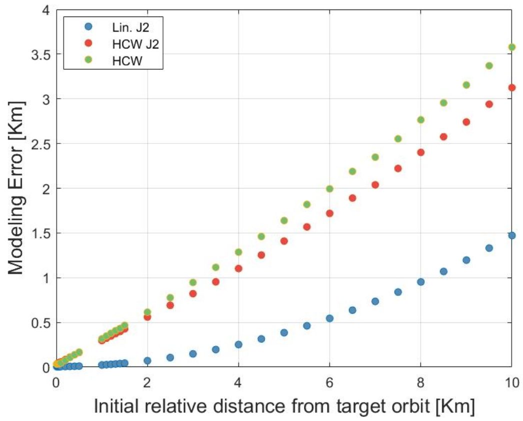

Fig. 1. Maximum modeling error of the three models - Linearized J2, HCW with and without J2 relative to high fidelity nonlinear model (7) – (9) for initial relative distance (LVLH frame) $[0.01, 15]$ km and simulation time length 5 orbital periods.

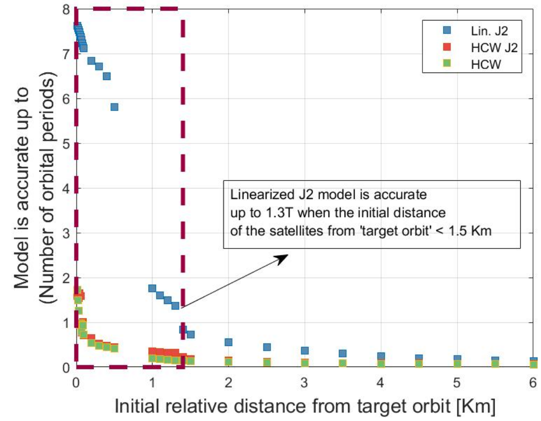

Fig. 2. Accuracy of the three models in terms of the length of time elapsed - linearized J2, HCW with and without J2 for initial relative distance (LVLH frame) $[0.01, 6]$ km. Corresponding to a specific initial distance, the figure shows the duration until which the trajectory error is smaller than 5 m and a model is deemed accurate.

C. Hill-Clohessy-Wiltshire (HCW) Model with J2

A modified HCW model considering earth's J2 non-spherical effect [11] is given as follows

$$\ddot{x}_j = a_{jx} + 2nc\dot{y}_j + (5k_1^2 - 2)n^2 x_j, \tag{14}$$

$$\ddot{y}_j = a_{jy} - 2nc\dot{x}_j, \tag{15}$$

$$\ddot{z}_j = a_{jz} - k_2^2 z_j, \tag{16}$$

where $k_2 = nk_1 + 1.5J_2\left(\frac{R_e \mathrm{c}_i}{r}\right)^2$, $k_1 = \sqrt{1+k_3}$, $k_3 = 0.375J_2\left(\frac{R_e}{r}\right)^2(1+3\mathrm{c}_{2i})$. In the absence of J2 perturbations, equations (14) – (16) reduce to original HCW model or popularly known as Hill's equation [20].

IV. Uncertainty quantification and modeling errors

In this section, we compare various dynamical models presented above and evaluate the modeling errors for numerous initial conditions. We are also interested to determine the time instant when the modeling errors go beyond a realistic position tolerance of 5 m [4]. For a given initial condition, we consider a model to be accurate till the time it is within this threshold value. This analysis helps us to determine which model should be used in the TO optimization for a given time window and initial relative position of satellites.

By solving (1)–(6), we obtain the time-series position, velocity and target orbit elements under J2 perturbation and air drag. With this target orbit data in (11) – (13) and in (14) – (16) we simulate the satellite trajectories in local frame for linearized J2 and HCW model (with and without J2) respectively. For a given initial position and simulation time window, the modeling error of the linearized J2 model is evaluated as the maximum relative distance between the trajectories generated by (11) – (13) and the nonlinear model (7) – (9) for the entire time. Modeling error for HCW with or without J2 are analogously computed with respect to the nonlinear model.

In Fig. 1, we present the maximum modeling errors of the three linear models relative to the high fidelity nonlinear model (7) – (9) under a sinusoidal actuation with frequencies within $[0, 1]$ rad s^{-1}, amplitudes between $[-3, 3]$ mN in a simulation for 5 orbital periods and initial positions drawn randomly from a uniform distribution such that the relative distance for these initial points from the origin lie between $[0.01, 15]$ km. Corresponding to a specific initial distance from the origin in LVLH frame, we randomly pick 150 initial positions, evaluate the maximum of modeling errors for these initial positions and replicate this approach for other initial relative distances and models. From Fig. 1, we observe that the linearized J2 model is more accurate as compared to the other models under considered sinusoidal actuation. We verified this to be true even when there is no actuation.

Next, we evaluate the duration in which all three models yield less than 5 m modeling error under aforementioned sinusoidal actuation. In addition to the modeling errors, we also evaluate the corresponding time instant when this model error exceeds beyond 5 m. The simulation results showing the accuracy of all three models are presented in Fig. 2 from which we observe again that, the linearized J2 model is more accurate than the rest. Precisely, when the initial distance from the target orbit is within 1.5 km, linearized J2 model error is within 5 m for more than one orbital period. Therefore by considering both the modeling error and accuracy time horizon, linearized J2 model is the most appropriate candidate to formulate the relative dynamics of satellite swarms in TO problem with initial distance within 1 km and final time $t_f = 1$ orbital period. For practical mission purposes, where the terminal time is more than one orbital period, we have to restart the TO problem in every one orbital period of time. For convenience, we denote an orbital period of time with T.

V. Formulation of the Basic TO Problem

This section presents the details of the MILP formulations to solve the basic TO problem as in [4], [5]. The core of this optimization problem is to select state variables $p_i(k) = \begin{bmatrix}\bar{p}_i(k) & \dot{\bar{p}}_i(k)\end{bmatrix}^{\mathrm{T}}, \bar{p}_i = \begin{bmatrix}x_i & y_i & z_i\end{bmatrix}^{\mathrm{T}}$, corresponding control $u_i(k)$ for each spacecraft $i = \{1, 2, \cdots, N\}$ satisfying Euler-discretized version of linearized J2 dynamics (11) – (13) with 1 second step size in the form

$$\begin{aligned} &p_i(k+1)=A(k)p_i(k)+Bu_i(k), k = 0, 1,\cdots,N_k-1 \\ &p_i(0) = p_{iS}, p_i(N_k) = p_{iD}, \end{aligned} \tag{17}$$

where p_{iS} and p_{iD} are respectively the initial and terminal state vectors for i^{th} spacecraft, and N_k is the terminal time step. Similar to [4], [5], we consider that inputs vectors with their respective slew rates lie within a specified limit

$$-u_{m,max} \leq u_{im}(k) \leq u_{m,max}, \; m = 1, 2, 3, \tag{18}$$

$$u^r_{m,min} \leq u_{im}(k+1)-u_{im}(k) \leq u^r_{m,max}, \tag{19}$$

where $u_{im}(k)$ denotes the m^{th} component of $u_i(k)$.

In contrast to traditional TO problems with well known final configuration [2], we consider that the assignment of the final configuration to each satellite is not known *a priori*. Assignment of final configuration is formulated as a mixed-integer linear constraints, given as follows

$$p_{iT} = \sum_{j=1}^{N} b_{ij} p_{jD}, \sum_{i=1}^{N} b_{ij} = 1, \sum_{j=1}^{N} b_{ij} = 1, \tag{20}$$

where the unity row sum and column sum of the assignment matrix $\mathcal{B} = [b_{ij}]_{N\times N}$ ensures that each of these terminal points $p_{iD}, \; i = 1, 2, \cdots, N$ is assigned to only one of the satellites. The objective of this TO problem is to minimize the total fuel consumption by all N satellites over the entire time horizon

$$\min_{u,p,\mathcal{B}} J = \sum_{i=1}^{N} \sum_{k=0}^{N_k-1} \sum_{m=1}^{3} |u_{im}(k)|$$

subject to (17) – (20). To illustrate this TO algorithm, we consider a simple numerical example with three satellites, starting from the origin at LVLH frame with $0.1 \mathrm{~m\,s^{-1}}$ radial velocity difference from one another, creating a "triangular" formation at $T/3$ and finally aligning themselves on a straight line with an inter-satellite separation distance of 478.75 metre at the final time T. The actuator saturation and rate limits are respectively 3 mN and 1 $\mathrm{mN\,s^{-1}}$. The optimal control law, within the specified actuation limits, renders the fuel optimal manuevers for the three satellites, shown in Figure 3 and the total fuel cost J is 22.8584.

However, solving this TO problem with a mixed-integer solver such as Gurobi [21] in a standard Windows computer (3.8 GHz CPU, 16 GB memory) takes nearly 8 minutes to compute optimal trajectories and control for three satellites. To improve the computationally efficiency with the current processing capabilities, we present in Section VI some alternative approaches to reformulate TO.

VI. Main Results

In Section V, we presented basic TO algorithm to obtain fuel optimal trajectories, controls and final assignment.

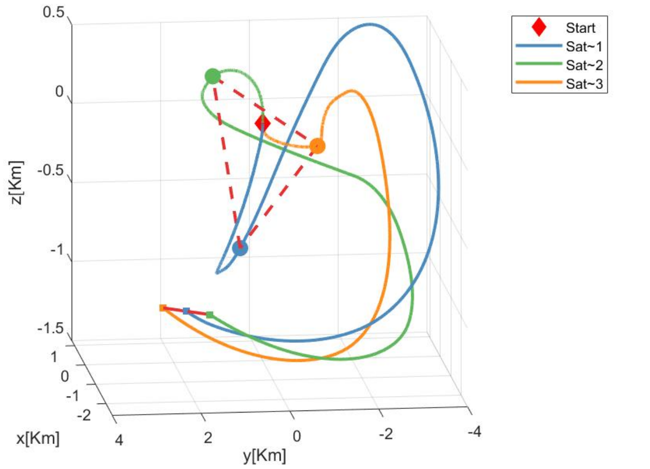

Fig. 3. Fuel optimal trajectories of the three satellites with the starting point marked with 'Diamond', intermediate triangular formation and final linear formations are shown with dashed red lines.

However, due to inclusion of N^2 binary variables associated with the final assignment constraint within the TO problem, computational complexity is prohibitive. In the proposed solution, we decouple the assignment problem and TO. The high-level idea is that, by solving a "transportation problem" [17], we derive a final configuration of satellites which are at the minimum overall distance from the initial formation assignment.

A. MILP formulation of the decoupled TO problem

The final configuration of satellites based on minimum distance assignment is formulated as

$$\textit{Assignment problem:} \min_{\mathcal{B}} J_D = \sum_{i=1}^{N} \sum_{j=1}^{N} d_{ij} b_{ij}$$

subject to

$$\sum_{i=1}^{N} b_{ij} = 1, \sum_{j=1}^{N} b_{ij} = 1,$$

where $d_{ij} = \|\bar{p}_{jD} - \bar{p}_{iS}\|_2$ denotes the distance between the i^{th} position of the initial formation and j^{th} of the final formation based on euclidean 2 norm, and b_{ij} is the $(i, j)^{\text{th}}$ element of the binary assignment matrix $\mathcal{B}$. This assignment algorithm, formulated as mixed-integer linear problem (MILP) is equivalent to well-known "transportation problem" where the objective is to find the path between a pair of initial and final points with minimum cost of transportation.

The solution to this optimization problem is the assignment matrix $\mathcal{B}$ that determines the final positions of N satellites. Given the final configuration of satellites $\bar{p}_{iD}, \; i = 1, 2, \cdots, N$, the structure of the decoupled fuel optimal TO problem is the same as the coupled counterpart in Section V, except for the objective function and final configuration constraint which no-longer have b_{ij} as one of the decision variables. Therefore, the objective function of the decoupled

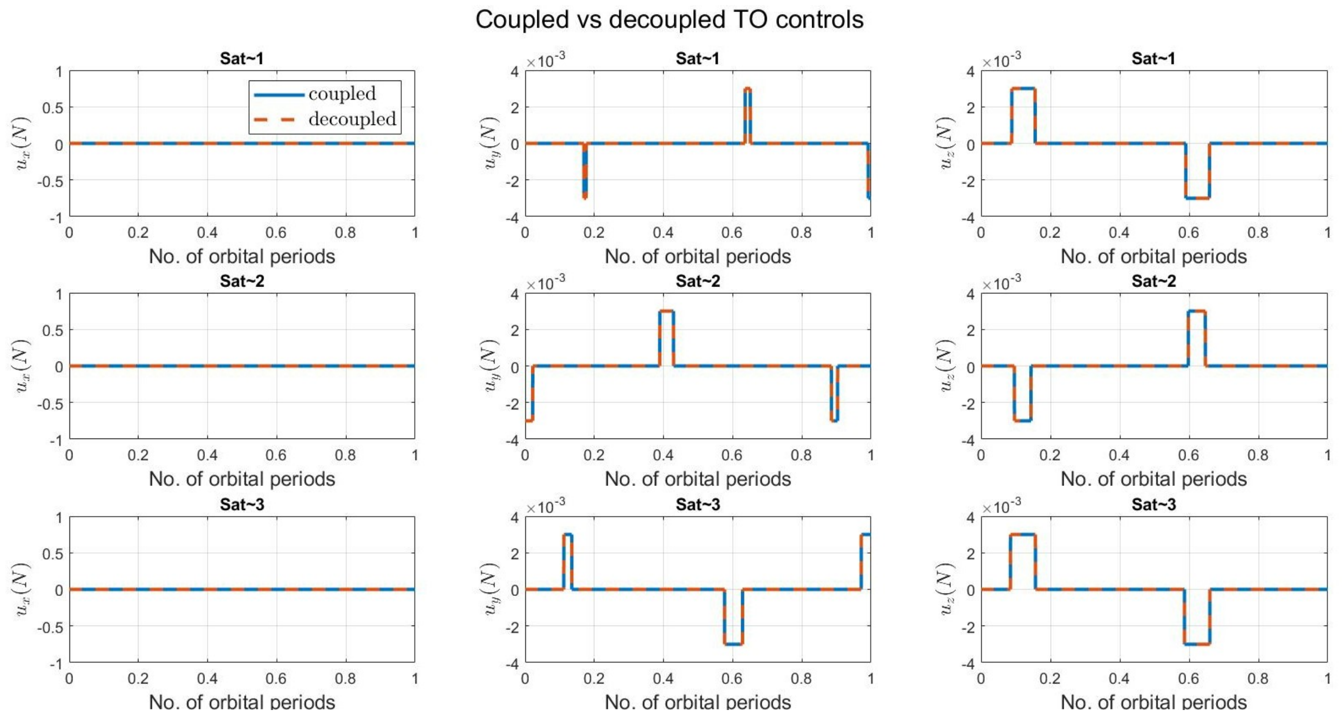

Fig. 4. Optimal control solution to coupled and decoupled TO problem in radial (u_x), along-track (u_y) and across-track (u_z) direction for three satellites.

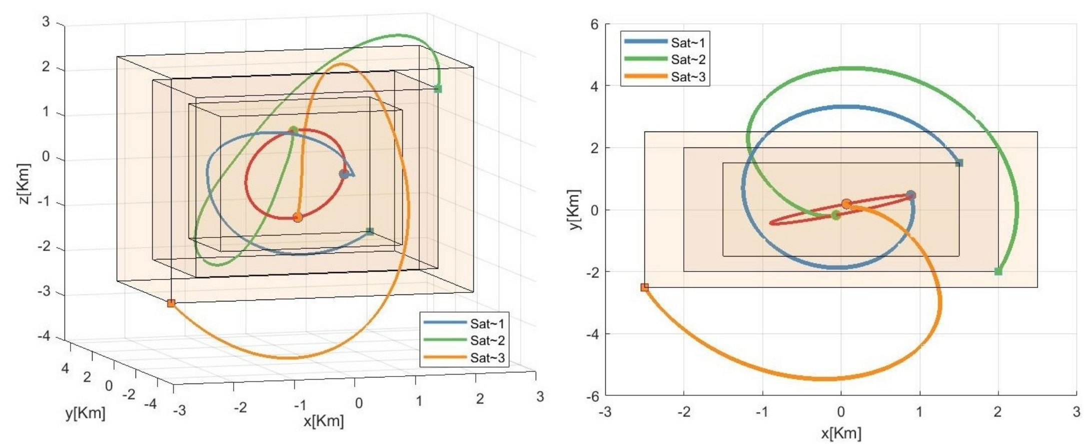

Fig. 5. Predicted fuel optimal trajectories for three satellites by the proposed TO algorithm .

TO problem thus becomes

$$\min_{u,p} \mathbf{J} = \sum_{i=1}^{N} \sum_{k=0}^{N_k-1} \sum_{m=1}^{3} |u_{im}(k)|$$

with the final position constraint $\bar{p}_{iT} = \sum_{j=1}^{N} b_{ij}\bar{p}_{jD}$, where b_{ij} is the solution to the *assignment problem*. We also note here, that the final position constrained can also be relaxed and put into the objective function with a large penalty to ensure feasibility, but we will not pursue that in this paper.

As we have decoupled the assignment problem, the resulting TO algorithm can now be solved by the swarm in a distributed manner. Hence, the computational load is significantly reduced with this decoupled TO formulation and it scales to any arbitrary swarm size. On the other hand, the assignment problem is solved in a centralized manner and therefore, it is of interest to investigate how scalable is this centralized optimization technique for assigning satellites. To illustrate this, let us present a numerical case study where we increase the swarm size from 1 to 500 in nonuniform sampling intervals with the satellites being initially located within 1 km distance and their final positions within 5 km distance from the origin in LVLH frame. For each formation size, we conduct 30 numerical case studies with different set of initial and final positions using standard Gurobi solver and evaluate the average of this computation times. The computational complexity of the assignment problem, thus calculated, is shown in Figure 6, from which we observe that the computational complexity increases almost quadratically with increasing swarm size.

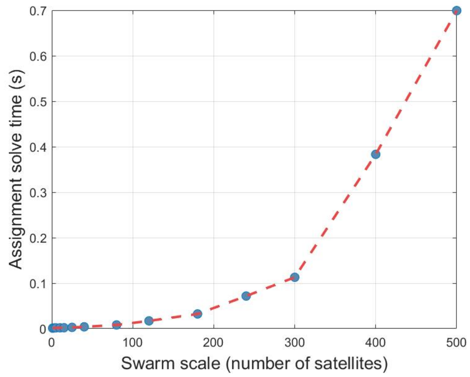

Fig. 6. Computational complexity of the assignment problem with increasing swarm size.

B. Illustrative example 1

Let us now consider a numerical example to illustrate the effectiveness of the decoupled TO problem as opposed to its coupled counterpart in Section V. Three satellites start from a unit disk around the origin in an LVLH frame and after one orbital period they are located on the vertices of the three cubes of edge lengths 3, 4 and 5 km using minimal fuel with available thrust limit being $3\ \mathrm{mN}$. In Section IV we demonstrated that the linearized J2 model used in TO algorithm is accurate for more than one orbital period when initial distance is less than $1.3\ \mathrm{km}$ and we thus purposefully selected the the satellites to be located at $1\ \mathrm{km}$ initial distance from the target orbit. We solve the fuel optimal TO problem using coupled TO algorithm based on minimum fuel assignment in Section V, and also with decoupled TO in VI-A which is based on minimum distance assignment, and consequently evaluate the predicted trajectory errors.

The optimal control solution and the trajectories for the TO problem are presented respectively in Figures 4, 5. We observe that the control solution is identical for both coupled and decoupled problem and so are the trajectories. Furthermore, the minimum distance assignment is same as the minimum fuel assignment. Solving this decoupled TO problem, formulated as MILP, in Gurobi for three satellites in a normal Windows computer took 40 seconds, which is nearly a tenth of the computation time for the coupled problem and hence decoupled TO in this case serves as an excellent alternative as far as the efficient trajectory planning is concerned.

Next we investigate whether these two assignments are identical for all formations and, if not, compute the loss of optimality as we move from the coupled TO algorithm based on minimum fuel assignment to decoupled TO based on the minimum distance assignment. Since the satellite dynamics have six coupled degrees of freedom and are governed by time-varying differential equations, it is not an easy task to analytically find a feasible space of initial and final points for which both the assignments are same. Therefore, our first attempt in this endeavor is to estimate numerically through Monte-Carlo simulations a probability distribution for identical assignment events and determine the relative fuel cost error between the coupled and decoupled TO problems when two assignments are different.

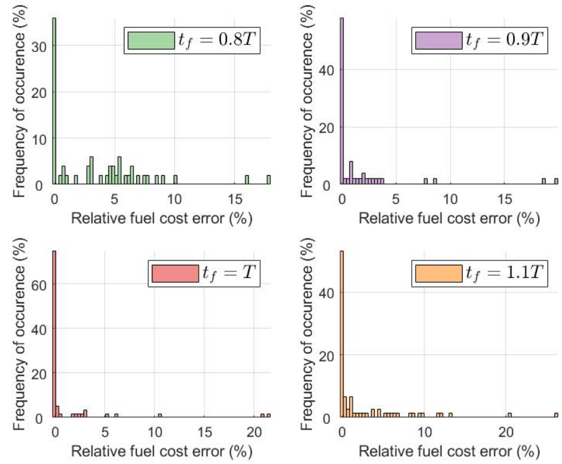

Fig. 7. Probability distribution of the relative fuel cost error between coupled and decoupled TO problem for different $t_f \in [0.8T, 1.1T]$ with mean $\mu = 3.5249,\ 1.6992,\ 1.3399,\ 2.45$ and standard deviation $\sigma = 4.08,\ 4.05,\ 4.14,\ 4.83$.

For these numerical simulations, we select initial and final positions from two uniform random distributions $\mathcal{U}(-1,1)\ \mathrm{km}$ and $\mathcal{U}(-5,5)\ \mathrm{km}$. Given the actuator saturation of $3\ \mathrm{mN}$ and rate limit $1\ \mathrm{mN\,s^{-1}}$, we select the final times t_f from the set $[0.8T, 1.1T]$ to arrive at a feasible solution to the TO problem satisfying all control constraints. If t_f is selected too small, for example $0.3T$ then to reach the destination in such a short period requires a large thrust which may be bigger than $3\ \mathrm{mN}$. Therefore, for this numerical case studies we purposefully select t_f's within $[0.8T, 1.1T]$.

For different t_f's, the relative fuel cost error between the coupled and decoupled TO problem and the associated probability distributions are given in Figure 7. For $t_f = 0.8T,\ 0.9T,\ T,\ 1.1T$, there are respectively 36%, 54.55%, 80% and 53.33% cases where minimum distance assignment is same as the minimum fuel assignment and associated relative fuel cost error is 0%. Clearly, as t_f tends to T, we numerically find that the solution to the decoupled TO problem is identical with its coupled counterpart for about 80% of cases. On either side of $t_f = T$, frequency of such occurrences decrease gradually. Nevertheless, for different t_f's, there are about 96% cases for which the decoupled fuel cost is at most 10% more than the coupled TO cost. Therefore, decoupled TO algorithm can be proposed as an alternative to the original TO problem for practical trajectory planning process while losing only 10% fuel optimality. However, there are nearly 4% cases in which the decoupled TO cost is 20% more than the coupled cost. To address this, one of our future works would be to include the curvature constraints in the decoupled TO problem.

Remark 1: In these works, we have implicitly assumed that the initial position and velocities of satellites are known accurately. In the presence of uncertainties associated with p_{iS}, the TO algorithm in the previous section, which was based on nominal initial positions, may in this case yield large trajectory prediction errors. Therefore, when x_{iS} is uncertain, a shrinking horizon optimal control is envisioned as a solution to address this issue and minimize the trajectory prediction errors. Specifically, to avoid accumulation of large modeling errors, we restart the TO algorithm after a small time interval (e.g., every 15 minutes) with new initial points that come from the high fidelity model (7) - (9) or real measurements, a representative of the actual fleet dynamics. This method of successive prediction and re-optimizing the TO with more accurate initial positions yields a more robust control profile that eventually renders a small trajectory prediction error in the face of uncertain initial positions. This shrinking horizon optimal control not only robustifies the TO against initial uncertainties and modeling errors, but also improves fuel-optimality with repeated optimization. Full investigation of this idea is an ongoing research topic.

VII. Conclusions

In this paper, we studied TO problem for SFF mission on circular or near-circular LEO under perturbations and modeling uncertainties. We reviewed several relative dynamical models of the satellites, and for various initial conditions and bounded actuation we evaluated the modeling errors which eventually allowed us to select the linearized J2 model as the most appropriate candidate for the TO algorithm.

Numerical simulations illustrate that the computational challenge of the TO algorithm is exacerbated by the presence of underlying final configuration assignment problem of the satellites. In this work, we proposed an alternative computationally-efficient approach to obtain near-optimal trajectories and actuation by using minimum distance assignment of satellites from initial to final formation at the expense of a small loss of fuel-optimality.

Our proposed future work includes introducing curvature constraints within the decoupled TO problem to further improve fuel optimality, studying the shrinking horizon optimal control approach discussed in Remark 1, and considering collision constraints within the TO.

Acknowledgement

The authors would like to thank Dr. Ryan McDevitt from Benchmark Space Systems and Dr. Amir Rahmani from NASA's Jet Propulsion Laboratory (JPL) for insightful discussions.

References

[1] D. Morgan, S.-J. Chung, L. Blackmore, B. Acikmese, D. Bayard, and F. Y. Hadaegh, "Swarm-keeping strategies for spacecraft under j2 and atmospheric drag perturbations," *Journal of Guidance Control and Dynamics*, vol. 35, no. 5, pp. 1492–1506, 2012.

[2] H. C. Lim and H. Bang, "Trajectory planning of satellite formation flying using nonlinear programming and collocation," *J. Astron. Space Sci.*, vol. 25, no. 4, pp. 361–374, 2008.

[3] I. Garcia and J. P. How, "Trajectory optimization for satellite reconfiguration maneuvers with position and attitude constraints," in *Proceedings of the 2005, American Control Conference, 2005.*, vol. 2, Portland, USA, 2005, pp. 889–894.

[4] M. Tillerson, G. Inalhan, and J. P. How, "Co-ordination and control of distributed spacecraft systems using convex optimization techniques," *Int. J. Robust Nonlinear Control*, vol. 12, pp. 207–242, 2002.

[5] A. Richards, T. Schouwenaars, J. P. How, and E. Feron, "Spacecraft trajectory planning with avoidance constraints using mixed-integer linear programming," *Journal of Guidance, Control, and Dynamics*, vol. 25, no. 4, pp. 755–764, 2002.

[6] R. Kristiansen and P. J. Nicklasson, "Spacecraft formation flying: A review and new results on state feedback control," *ACTA Astronautica*, vol. 65, pp. 1537–1552, 2009.

[7] D. P. Scharf, F. Y. Hadaegh, and S. R. Ploen, "A survey of spacecraft formation flying guidance and control (part i): Guidance," in *in Proc. of the American Control Conference*, Denver, Colorado, USA, 2003, pp. 1733–1739.

[8] C. W. T. Roscoe, J. D. Griesbach, J. J. Westphal, D. R. Hawes, and J. J. P. Carrico, "Force modeling and state propagation for navigation and maneuver planning for cubesat rendezvous, proximity operations, and docking," *Advances in the Astronautical Sciences*, vol. 150, pp. 573–590, 2014.

[9] M. Eshagh and M. N. Alamdari, "Perturbations in orbital elements of a low earth orbiting satellite," *Journal of the Earth & Space Physics.*, vol. 33, no. 1, pp. 1–12, 2007.

[10] G. Inalhan and J. How, "Relative dynamics and control of spacecraft formations in eccentric orbits," *Journal of Guidance, Control, and Dynamics*, vol. 25, no. 1, pp. 48–59, 2002.

[11] J. Ma, "Formation flying of spacecrafts for monitoring and inspection," Master's thesis, Lulea University of Technology, Sweden, 2009.

[12] G. Xu and D. Wang, "Nonlinear dynamic equations of satellite relative motion around an oblate earth," *Journal of Guidance, Control and Dynamics*, vol. 31, no. 5, pp. 1521–1524, 2008.

[13] I. Khalil and S. Samwel, "Effect of air drag force on low earth orbit satellites during maximum and minimum solar activity," *Space Research Journal*, vol. 9, pp. 1–9, 2016.

[14] S. Schweighart and R. Sedwick, "High-fidelity linearized j2 model for satellite formation flight," *Journal of Guidance, Control, and Dynamics*, vol. 25, no. 6, pp. 1073–1080, 2002.

[15] J.-F. Hamel and J. D. Lafontaine, "Linearized dynamics of formation flying spacecraft on a j2-perturbed elliptical orbit," *Journal of Guidance, Control, and Dynamics*, vol. 30, no. 6, pp. 1649–1658, 2007.

[16] D. Wang, B. L. Wu, and E. K. Poh, *Satellite Formation Flying*, ser. Intelligent Systems, Control and Automation: Science and Engineering. Singapore: Springer, 2017, vol. 87.

[17] A. Chaudhuri and K. De, "A comparative study of transportation problem under probabilistic and fuzzy uncertainties," *CoRR*, vol. abs/1307.1891, 2013. [Online]. Available: http://arxiv.org/abs/1307.1891

[18] A. F. R. L. S. V. Directorate, "Techsat 21 factsheet page," https://www.vs.afrl.af.mil/factsheets/TechSat21.html, 2019, online; accessed 8 September 2021.

[19] B. Wu, G. Xu, and X. Cao, "Relative dynamics and control for satellite formation: Accommodating j2 perturbation," *Journal of Aerospace Engineering*, vol. 29, no. 4, p. 04016011, 2016.

[20] M. Sidi, *Spacecraft Dynamics & Control: A Practical Engineering Approach*, ser. Cambridge Aerospace Series. Cambridge University Press, 2006, vol. 7.

[21] Gurobi Optimization, LLC, "Gurobi Optimizer Reference Manual," 2021. [Online]. Available: https://www.gurobi.com